HHS Public Access

Author manuscript

Spine (Phila Pa 1976). Author manuscript; available in PMC 2023 January 01.

Published in final edited form as:

Spine (Phila Pa 1976). 2022 January 01; 47(1): 82–89. doi:10.1097/BRS.0000000000004142.

Preclinical Safety of a 3D-Printed Hydroxyapatite-Demineralized Bone Matrix Scaffold for Spinal Fusion

Mark Plantz, BS[a,b], **Joseph Lyons, BS**[a,b], **Jonathan T. Yamaguchi, MS**[a,b], **Allison C. Greene, BS**[a,b], **David J. Ellenbogen, BA**[a,b], **Mitchell J. Hallman, BA**[a,b], **Vivek Shah, BS**[a,b], **Chawon Yun, PhD**[a,b], **Adam E. Jakus, PhD**[c], **Daniele Procissi, PhD**[d], **Silvia Minardi, PhD**[a,b], **Ramille N. Shah, PhD**[b,c], **Wellington K. Hsu, MD**[a,b], **Erin L. Hsu, PhD**[a,b]

[a]Department of Orthopaedic Surgery, Northwestern University, Chicago, IL;

[b]Center for Regenerative Nanomedicine, Simpson Querrey Institute, Chicago, IL;

[c]Dimension Inx Corp, Chicago, IL;

[d]Department of Radiology, Northwestern University, Chicago, IL.

Abstract

Study Design.—Prospective, randomized, controlled preclinical study.

Objective.—The objective of this study was to compare the host inflammatory response of our previously described hyperelastic, 3D-printed (3DP) hydroxyapatite (HA)-demineralized bone matrix (DBM) composite scaffold to the response elicited with the use of recombinant human bone morphogenetic protein-2 (rhBMP-2) in a preclinical rat posterolateral lumbar fusion model.

Summary of Background Data.—Our group previously found that this 3D-printed HA-DBM composite material shows promise as a bone graft substitute in a preclinical rodent model, but its safety profile had yet to be assessed.

Methods.—Sixty female Sprague-Dawley rats underwent bilateral posterolateral intertransverse lumbar spinal fusion using with the following implants: 1) type I absorbable collagen sponge (ACS) alone; 2) 10 μg rhBMP-2/ACS; or 3) the 3DP HA-DBM composite scaffold (n = 20). The host inflammatory response was assessed using magnetic resonance imaging, while the local and circulating cytokine expression levels were evaluated by enzyme-linked immunosorbent assays at subsequent postoperative time points (N = 5/time point).

Results.—At both 2 and 5 days postoperatively, treatment with the HA-DBM scaffold produced significantly less soft tissue edema at the fusion bed site relative to rhBMP-2-treated animals as quantified on magnetic resonance imaging. At every postoperative time point evaluated, the level of soft tissue edema in HA-DBM-treated animals was comparable to that of the ACS control group. At 2 days postoperatively, serum concentrations of tumor necrosis factor-α and macrophage chemoattractant protein-1 were significantly elevated in the rhBMP-2 treatment group

Address correspondence and reprint requests to Erin L. Hsu, PhD, Robert H Lurie Medical Research Center Room 11-107, 303 E Superior, Chicago, IL 60611; erinkhsu@gmail.com.

The device(s)/drug(s) that is/are the subject of this manuscript is/are not intended for human use.

relative to ACS controls, whereas these cytokines were not elevated in the HA-DBM-treated animals.

Conclusion.—The 3D-printed HA-DBM composite induces a significantly reduced host inflammatory response in a preclinical spinal fusion model relative to rhBMP-2.

Level of Evidence: N/A

Keywords

3D printing; bone morphogenetic protein-2; demineralized bone matrix; host inflammatory response; hydroxyapatite; spinal fusion

Spinal arthrodesis is an established and reliable treatment for a number of spinal conditions and remains among the most common surgical procedures performed worldwide.[1–3] Despite its success however, pseu-darthrosis, or surgical nonunion, remains a significant challenge. Failure to achieve a solid fusion may result in poor clinical outcomes and extensive medical expenditure, motivating substantial efforts aimed at developing strategies to avoid this frustrating complication.[4–6] While autogenous bone graft is generally effective for fusion, its procurement can cause significant morbidity and postoperative pain and is limited in available volume.[7–9] Recombinant human bone morphogenetic protein-2 (rhBMP-2) was initially thought to provide the optimal solution, resulting in high rates of fusion without the requirement for autogenous bone harvest.[10] However, its widespread adoption as a bone graft substitute has since spawned a number of safety concerns surrounding its use.[11–13]

The ongoing search for a material that is both safe and ideally suited to optimize bone formation for fusion has resulted in a number of innovative strategies and technologies that show significant promise.[14,15] When evaluating such technologies for potential clinical application, a fundamental knowledge of the biological responses elicited upon implantation is critical to establishing both efficacy and safety.[16] Experience with the use of high-dose recombinant growth factors such as rhBMP-2 in the setting of spine surgery has shown that in addition to osteoinductive capacity, a careful assessment of the host inflammatory response is necessary to validate its safety.[17,18] There are several *in vitro* and *in vivo* cell-based models that may be used to better understand the host reaction to a new material; however, the specificity of such tests may be limited.[19–23] A number of factors, such as the anatomic site of implantation, can influence how a biomaterial alters the normal inflammatory reaction process.[24] Therefore, an animal model that closely resembles the conditions of the intended application is desirable to more accurately gauge potential safety concerns.

Our group previously reported the implementation of a modified rodent posterolateral spine fusion (PLF) model which successfully replicated the host inflammatory response to rhBMP-2 observed clinically.[25] In this model, rhBMP-2-treated animals develop a postoperative fluid collection observable on high-resolution magnetic resonance (MR) imaging as well as disproportionate elevations of certain proinflammatory and osteoclastic cytokines in the serum. We postulated that this mechanism of action could lead to the clinical complications reported in the literature. The purpose of the current study was to characterize the host inflammatory response to our recently developed 3D-printed HA-DBM

composite scaffold using temporal quantification of local fluid collection as well as local and circulating cytokine production using this modified PLF model.

MATERIALS AND METHODS

Study Design

Sixty female Sprague-Dawley rats, ages 12 to 16 weeks, underwent a bilateral posterolateral intertransverse lumbar spinal fusion using one of three implants: 1) type I absorbable collagen sponge (ACS) alone (negative control, n = 20), 2) 10 μg rhBMP-2/ACS (positive control; 0.075 mL rhBMP-2 per ACS scaffold, at 0.067 mg/mL final per side; n = 20), or 3) HA-DBM composite scaffold (n = 20). This standard dose of 10 μg rhBMP-2 was chosen because it produces a fusion rate of 100% in this preclinical model.[26,27] Institutional Animal Care and Use Committee approval at Northwestern University was obtained for this work, under protocol number 2016 to 2610 and with an Animal Welfare Assurance with the Office of Laboratory Animal Welfare (A3283-01).

Scaffold Fabrication

The scaffold being evaluated in this work is a hyperelastic, 3D-printed composite biomaterial which we developed for use in the spine fusion setting. Scaffold design was based on our previous work which established both the ink composition and scaffold geometry/architecture which produced high rates of fusion in the rat model.[28,29] The HA-DBM ink was produced using our previously described protocols.[28–30] Briefly, the ink was composed of 30 vol.% polylactide-co-glycolide (PLG; 82:18 glycolide to lactide) copolymer (Evonik Cyro) and 70 vol.% of HA + DBM particles. The particle component comprised a ratio of three parts of HA to one part of DBM. Medical-grade synthetic HA powder (particle diameter range of ~1–25 μm) was provided by Merz North America. DBM particles (~100–1000 μm) were provided by Xtant Medical (Belgrade, MT), and were milled to a range of 20 to 80 μm diameter. The scaffolds were printed using a 3D-Bioplotter (EnvisionTEC, Germany) using a 410 μm diameter nozzle with a syringe extrusion system at room temperature. Scaffolds five layers thick were printed with previously optimized architectural parameters: each successive layer of struts was laid at 45° relative to the underlying layer, and the edge-to-edge strut spacing was 1000 μm.[29] After printing, the scaffolds were washed with 70% ethanol followed by sterile phosphate-buffered saline and trimmed to a uniform size (15 × 4 × 3 mm) prior to implantation.

Posterolateral Fusion Model for Evaluation of Inflammation

The host inflammatory response to rhBMP-2 akin to that observed clinically was reproduced in a modified rat PLF model as we have previously described.[25,31] Briefly, under continuous anesthesia with an isoflurane inhalational anesthetic delivery system, two separate fascial incisions were made 4 mm from the midline exposing the L4 and L5 transverse processes. The overlying lumbar paraspinal muscular compartment was resected *en bloc* bilaterally to create a voided space adjacent to the spine. Total paraspinal muscle tissue resection weight averaged 0.84 ± 0.15 g per animal. The surgical site was irrigated with gentamicin solution, and the fusion bed between the L4 and L5 transverse processes was then prepared as for a typical PLF procedure. After decortication with an oscillating burr, the graft materials were

implanted to bridge the L4 to L5 transverse processes. Fascial incisions were closed with the use of a 3–0 polyglactin absorbable running suture (Vicryl; Ethicon, Inc, Somerville, NJ). Five mL lactated Ringer solution was administered intraperitoneally after wound closure for hydration support. Rats were maintained on a heating pad and monitored continuously until ambulatory, and then every 15 minutes for the first hour after surgery. Buprenorphine sustained-release (0.03 mg/kg) was administered subcutaneously to provide analgesia for up to 72 hours postoperatively. Additionally, meloxicam was administered (1–2 mg/kg) SQ every 24 hours for 3 days. All animals recovered successfully from surgery and no postoperative complications were noted.

Magnetic Resonance Imaging and Analysis

Soft tissue edema volume on magnetic resonance imaging (MRI) was measured as an index of inflammation after surgical implantation of the materials. Animals were euthanized using a bilateral thoracotomy technique at 2 days, 5 days, 10 days, and 8 weeks after surgery. To ensure that the mean time from surgery to the time of MRI was uniform among the three groups, the animals underwent MRI in the same order that they underwent the surgery. Although we previously found postoperative fluid collections to be significantly higher in rhBMP-2-treated animals relative to ACS controls out to only 10 days, the inclusion of PLG in the HA-DBM scaffold composition, which has a significantly longer degradation period, warranted quantification out to a later timepoint. A 7T Clinscan MRI scanner (Bruker, Ettlingen, Germany) using a quadrature volume transceiver coil was used for all MRI scans to obtain T1- and T2-weighted sagittal and axial lumbar spine images. All the scans were performed with a 150-mm field of view, 0.9-mm slice thickness, and repetition time/echo time = 5940/62 and 600/12 ms for T2- and T1-weighted scans, respectively. Each scan was performed with an external water reference, which was used for normalization of signal intensity across the data sets to permit reliable and reproducible analysis. Intensity normalization was performed using Jim software (Version 8, Xinapse Systems Ltd, Colchester, UK) by manually sampling regions of interest within the water references and using the mean intensity within the regions of interest as a reference to linearly scale the images. The volume of soft tissue edema was then quantified from the normalized T2-weighted MR images using open-source 3D Slicer software (Version 4.10.2, The Brigham and Women's Hospital, Inc, Boston, MA).[32] The region corresponding to the fusion bed was isolated on all scans using manual segmentation to ensure that unrelated edema—such as from the incision itself—was excluded from the volume calculations. From the isolated region, the edema volume was then quantified using a standardized intensity threshold-based automatic segmentation (Figure 1).

Histological Evaluation

At each study endpoint, implants were harvested and fixed in 10% formalin buffer for 7 days. They were then transferred to a 50% ethanol solution for 2 hours, followed by storage in 70% ethanol. Samples were demineralized in 10% HCl solution for 8 hours. Samples were then processed and embedded in paraffin by the Northwestern University Mouse Histology & Phenotyping Laboratory core. 7-μm-thin sections were cut with a RM2255 microtome (Leica). Sections were deparaffinized and rehydrated by immersing the slides through the following solutions: xylene (three washes 5 min each), 100% ethanol (two

washes 5 min each), ethanol solutions (95%, 90%, 80%, 70%, and 50% in distilled water), and distilled water. Sections were stained with Gill's hematoxylin and eosin and alcian blue according to the manufacturer's recommendations (Sigma Aldrich). Stained sections were mounted with Cytoseal XYL mounting medium (Thermo Scientific), imaged on a TissueGnostic histological microscope (Zeiss), and visualized using TissueFAXS software.

Serum Cytokine Analysis

At 2-, 5-, and 10- days postoperatively, animals underwent blood collection *via* cardiac puncture under anesthesia, prior to euthanasia by bilateral thoracotomy. Whole blood was centrifuged at 10,000 × g for 10 minutes, and the serum (supernatant) was collected and stored at −80°C. Enzyme-linked immunosorbent assays (ELISA) were performed to quantify the serum levels of the five cytokines previously found to be induced in rhBMP-2-treated animals: interleukin (IL)-18, IL-1β, tumor necrosis factor (TNF)-α, macrophage inflammatory protein (MIP)-1α, and macrophage chemoattractant protein (MCP)-1.[25] Five biological samples per experimental group were tested, which were each quantified in technical duplicates. Rat DuoSet ELISA Development System kits (R&D Systems) were used according to the manufacturer's specifications, and absorbance was measured at 450 nm.

Statistical Analysis

All values were reported as the mean ± SD. A power analysis using a previously collected data set showed that a sample size of 5 at each time point was sufficient to detect statistical significance with $\alpha = 0.05$ and 80% power.[25] Statistical analysis was performed using IBM SPSS Statistics for Windows, version 23 (IBM Corp, Armonk, NY). Differences in edema volume measurements on MRI were determined using a one-way analysis of variance (ANOVA) and *post-hoc* Tukey's HSD (honestly significant difference) test. ELISA data were analyzed with a one-way analysis of variance and a Tukey's multiple comparison test with GraphPad Prism 8. In all analyses, statistical significance was considered with $P < 0.05$ (* $P < 0.05$, ** $P < 0.01$, *** $P < 0.001$).

RESULTS

A local inflammatory response—as evidenced by increased signal at the fusion bed on T2-weighted MR images—was observed in the early postoperative period in all treatment groups (Figure 2). This response was expected after any surgical insult. However, free fluid collections which formed at the surgical site and were most apparent at 2 days postoperatively remained incompletely resolved in the rhBMP-2 treatment group out to 10 days; this prolonged effect was not seen in either the ACS controls or the HA-DBM treatment group (Figure 2).

The inflammatory edema volume reached a peak at 2 days postoperatively in all treatment groups, with a gradual decrease in response at each time point thereafter (Figure 3). However, edema volumes were greater in the rhBMP-2 group relative to both the ACS and HA-DBM groups at all postoperative timepoints, although statistically significant differences were observed only in the early postoperative period. At 2 days postoperatively,

rhBMP-2-treated animals demonstrated a mean inflammatory volume of 1756 ± 377 mm^3 within the fusion bed, which was significantly greater than that of both ACS-treated (774 ± 270 mm^3) and HA-DBM-treated (610 ± 185 mm^3) animals ($P < 0.05$). By 5 days, MRI demonstrated decreasing inflammatory volumes in all the treatment groups, although these remained highest in the rhBMP-2 group (ACS, 738 ± 157 mm^3; rhBMP-2, 882 ± 118 mm^3; HA-DBM, 516 ± 149 mm^3) ($P < 0.05$). Statistically significant differences were no longer observed among treatment groups at the 10-day timepoint (ACS, 180 ± 89 mm^3; rhBMP-2, 404 ± 281 mm^3; HA-DBM, 134 ± 32 mm^3). By 8 weeks postoperatively the MRI signal changes were resolved in all the groups (ACS, 0.7 ± 0.7 mm^3; rhBMP-2, 8.4 ± 8 mm^3; HA-DBM, 6.2 ± 8.7 mm^3), indicating full recovery from the surgical insult, regardless of implant type. Notably, there were no significant differences in inflammatory edema volumes between the ACS and HA-DBM groups at any of the postoperative timepoints measured.

Histological evaluation did not show any abnormal tissue morphology or exacerbated cell infiltration in HA-DBM compared with ACS controls (Figure 4). More infiltrating cells were found in rhBMP-2 at 2, 5, and 10 days compared with ACS and HA-DBM. Collagen bundles were evident up to 10 days postoperatively in both ACS and rhBMP-2 (indicated by yellow arrows). ACS was fully resorbed by 8 weeks, while new trabecular bone-like tissue replaced the rhBMP-2 scaffold. New tissue was found in between the struts of HA-DBM, after 5 days postoperatively, and without apparent signs of edema.

rhBMP-2 treatment resulted in significantly increased expression of several cytokines at various time points relative to the negative control group (*e.g.*, ACS)—IL-1β at 2, 5, and 10 days postoperatively, TNF-α at 2 days postoperatively, MIP-1 at 2 days postoperatively, and MCP-1 at 2 and 5 days postoperatively ($P < 0.05$ for all) (Figure 5 and Table 1). Additionally, HA-DBM treatment resulted in a significantly increased expression of several cytokines relative to the ACS group—IL-1β at 2, 5, and 10 days postoperatively, IL-18 at 2 and 5 days postoperatively, and MIP-1 at 2 days postoperatively. Additionally, the relative expression of MCP-1 was greater in the rhBMP-2 group relative to the HA-DBM group at days 5 and 10 postoperatively. The relative expression of IL-18 was greater in the HA-DBM group relative to the rhBMP-2 group at 5days postoperatively.

DISCUSSION

In previous work, we developed and described a novel 3D-printed HA-DBM composite biomaterial which showed efficacy for promoting bone regeneration and spine fusion in a preclinical rodent model.[28,29] There, we showed that HA-DBM achieved a fusion rate of 92%.[28] However, its biocompatibility and safety profile have not been assessed in this setting. Such evaluations are critical prerequisites for successful translation from bench to bedside. For example, the scaffold utilized in this study is fabricated using a PLG copolymer, one of the most common polymer systems used in bone tissue engineering applications.[33–35] Although minimal systemic toxicity is associated with the use of PLG for biomaterial applications, its degradation products are acidic and there exists the concern that these byproducts could induce a local inflammatory response, potentially interfering with the key biological processes involved in new bone matrix deposition and tissue regeneration.[36–38] Furthermore, while several studies have investigated the toxicity and

biocompatibility of similar composite materials, the investigation of the host inflammatory response to these materials in a relevant preclinical model of spinal fusion has not been undertaken.[39,40] Therefore, the current study was designed to evaluate the host inflammatory response elicited by the HA-DBM material *via* temporal quantifications of fluid collection and cytokine expression in a previously established preclinical small animal model of spine fusion.[25,26,29] This model is relevant when considering the potential spine surgery applications of a new implant material, as it closely reproduces the fusion environment. As this is a surgical model, some degree of postoperative inflammation would be expected due simply to surgical insult. As a baseline negative control to account for any surgery-induced inflammation independent of a bioactive implant, ACS served as the negative control, since it is osteoinductively inert. rhBMP-2, which is known to cause a substantial pro-inflammatory response, served as the positive control.[25] Our previous work characterized the host response to high-dose rhBMP-2/ACS in this model,[25] making this an ideal comparative for this preclinical safety assessment of the HA-DBM scaffold. MRI analyses served to quantify the magnitude of the local inflammatory response, while serum cytokine analysis was used to identify any potential systemic effects.

Quantitative MRI found that the HA-DBM treatment produced significantly less edema relative to rhBMP-2/ACS—a nearly 3-fold decrease in inflammatory volume within the fusion bed at 2 days postoperatively. Additionally, the local inflammatory response as quantified on MRI did not differ significantly between the HA-DBM treatment and the ACS (negative control) treatment at any postoperative time point. Consistent with other studies utilizing similar MRI-based methodology, rhBMP-2 treatment was found to elicit a significant inflammatory response peaking in the early postoperative period and subsequently decreasing at later timepoints.[41–44] The magnitude of the inflammatory response in the ACS and HA-DBM groups was less than that of rhBMP-2 at all timepoints. Despite the fact that the HA-DBM group contained PLGA, which can be inflammatory[36–38] and was not degraded by the study endpoint, there was no prolonged inflammation seen in this treatment group. Therefore, the amount of PLGA in the implants were not sufficient to induce a prolonged inflammatory response. As expected, there was minimal quantifiable edema in any treatment group at 8 weeks postoperatively. The final time point of 8 weeks was chosen as this is the most commonly used endpoint for assessment of successful fusion in the L4-L5 posterolateral fusion model in rodents.[28,29]

The cytokine analysis revealed trends which were somewhat similar to those observed from imaging data. Treatment with rhBMP-2 was found to elicit significant elevations in the expression of multiple cytokines of interest in the immediate postoperative period which was consistent with previous findings.[25] IL-1β, TNF-α, MIP-1, and MCP-1 – all proinflammatory cytokines previously found implicated in the host response to rhBMP-2[25] —were indeed significantly elevated in the rhBMP-2 group, when compared with the ACS negative control group at early postoperative time points. In the current study, however, no significant elevation in IL-18 expression was noted in the rhBMP-2 group relative to the ACS group. It should be noted that our previous worked evaluated a 10-fold higher dose of rhBMP-2, which could reasonably explain the less substantial expression of various cytokines demonstrated in the current study. HA-DBM treatment did produce significant increases in the expression of certain cytokines – IL-1β, IL-18, and MIP-1 – at different

time points relative to the ACS negative control group. However, unlike the rhBMP-2 group, the HA-DBM group did not yield increased expression of TNF-α nor MCP-1 at any postoperative time points. This suggests that rhBMP-2 treatment yielded IL-1β-induced production of MCP-1 and a subsequent inflammatory response – something that was not seen with the ACS or HA-DBM treatment groups. Furthermore, MCP-1 has been associated with recruitment of monocytes, which can be pro-inflammatory when activated by IL-1β.[45] Prior studies have also reported upregulation of osteoclastogenesis in the setting of rhBMP-2[46] and MCP-1 is known to be an important upregulator of osteoclast activity.[47] These findings further corroborate potential cellular signaling pathways that explain bone resorption seen with the use of rhBMP-2 in the clinical setting.

While this model may provide valuable insights into the host inflammatory response to novel biomaterials intended for spine surgery applications, there are limitations to the current study which should be considered in context of the results. Given the use of a rodent model, the dose of rhBMP-2 used in this study is significantly lower than that required to achieve fusion in human subjects, and the findings in this study should be interpreted in that context. Furthermore, the current investigation was limited to the lumbar spine fusion environment. This may limit conclusions regarding the safety of a new material from being extrapolated to the cervical spine as the inflammatory response may not be identical at both locations. However, since there exists no small animal cervical spine fusion model, further studies implementing this experimental design in the cervical spine of larger animals will be necessary to make such comparisons in that setting. Lastly, the effects of surgical manipulation and paraspinal muscle resection on inflammation was not quantified relative to a nonoperative control group. However, the same surgical technique was used for the ACS control group, so the relative difference in inflammation was attributed to the material properties.

Despite these limitations, the collective results of the current investigation demonstrate the HA-DBM composite scaffold material to elicit a host inflammatory response of significantly lower magnitude relative to rhBMP-2. Furthermore, the host response to the HA-DBM did not generally differ from that which was elicited by ACS alone, suggesting that it may indeed be a safer alternative bone graft substitute to rhBMP-2 in this clinical setting.

CONCLUSION

Based on these preliminary findings, the HA-DBM composite material demonstrates a favorable biocompatibility profile, and further investigation of the material as a bone graft substitute in spinal fusion is warranted. Future investigation could assess the degradation and clearance rate of this material and any impact that this may have on clinical efficacy and biocompatibility.

Acknowledgments

This project was supported by the National Institute of Arthritis and Musculoskeletal and Skin Diseases (5R01AR069580-04). Imaging work was performed at the Northwestern University Center for Advanced Microscopy, which is supported by NCI CCSG P30 CA060553, awarded to the Robert H Lurie Comprehensive Cancer Center. A portion of the biochemical analysis was performed using instruments in the Analytical bioNanoTechnology Core Facility of the Simpson Querrey Institute at Northwestern University. ANTEC

is currently supported by the Soft and Hybrid Nano-technology Experimental (SHyNE) Resource (NSF ECCS-2025633).

Relevant financial activities outside the submitted work: grants, employment.

References

1. Herkowitz HN, Kurz LT. Degenerative lumbar spondylolisthesis with spinal stenosis. A prospective study comparing decompression with decompression and intertransverse process arthrodesis. J Bone Joint Surg Am 1991;73:802–8. [PubMed: 2071615]
2. Resnick DK, Watters WC 3rd, Sharan A, et al. Guideline update for the performance of fusion procedures for degenerative disease of the lumbar spine. Part 9: lumbar fusion for stenosis with spondylolisthesis. J Neurosurg Spine 2014;21:54–61. [PubMed: 24980586]
3. Martin BI, Mirza SK, Spina N, et al. Trends in lumbar fusion procedure rates and associated hospital costs for degenerative spinal diseases in the United States, 2004 to 2015. Spine (Phila Pa 1976) 2019;44:369–76. [PubMed: 30074971]
4. Makino T, Kaito T, Fujiwara H, et al. Does fusion status after posterior lumbar interbody fusion affect patient-based QOL outcomes? An evaluation performed using a patient-based outcome measure. J Orthop Sci 2014;19:707–12. [PubMed: 24916199]
5. Makino T, Kaito T, Fujiwara H, et al. Risk factors for poor patient-reported quality of life outcomes after posterior lumbar interbody fusion: an analysis of 2-year follow-up. Spine (Phila Pa 1976) 2017;42:1502–10. [PubMed: 28248893]
6. Tsutsumimoto T, Shimogata M, Yoshimura Y, et al. Union versus nonunion after posterolateral lumbar fusion: a comparison of long-term surgical outcomes in patients with degenerative lumbar spondylolisthesis. Eur Spine J 2008;17:1107–12. [PubMed: 18536941]
7. Banwart JC, Asher MA, Hassanein RS. Iliac crest bone graft harvest donor site morbidity. A statistical evaluation. Spine (Phila Pa 1976) 1995;20:1055–60. [PubMed: 7631235]
8. Dimitriou R, Mataliotakis GI, Angoules AG, et al. Complications following autologous bone graft harvesting from the iliac crest and using the RIA: a systematic review. Injury 2011;42 (suppl 2):S3–15.
9. Gruskay JA, Basques BA, Bohl DD, et al. Short-term adverse events, length of stay, and readmission after iliac crest bone graft for spinal fusion. Spine (Phila Pa 1976) 2014;39:1718–24. [PubMed: 24979140]
10. Zlotolow DA, Vaccaro AR, Salamon ML, et al. The role of human bone morphogenetic proteins in spinal fusion. J Am Acad Orthop Surg 2000;8:3–9. [PubMed: 10666648]
11. Smucker JD, Rhee JM, Singh K, et al. Increased swelling complications associated with off-label usage of rhBMP-2 in the anterior cervical spine. Spine (Phila Pa 1976) 2006;31:2813–9. [PubMed: 17108835]
12. Carragee EJ, Ghanayem AJ, Weiner BK, et al. A challenge to integrity in spine publications: years of living dangerously with the promotion of bone growth factors. Spine J 2011;11:463–8. [PubMed: 21729794]
13. Carragee EJ, Hurwitz EL, Weiner BK. A critical review of recombinant human bone morphogenetic protein-2 trials in spinal surgery: emerging safety concerns and lessons learned. Spine J 2011;11:471–91. [PubMed: 21729796]
14. Kumar S, Nehra M, Kedia D, et al. Nanotechnology-based biomaterials for orthopaedic applications: recent advances and future prospects. Mater Sci Eng C Mater Biol Appl 2020;106:110154. [PubMed: 31753376]
15. Sharma B, Varghese S. Progress in orthopedic biomaterials and drug delivery. Drug Deliv Transl Res 2016;6:75–6. [PubMed: 26935432]
16. Zhou G, Groth T. Host responses to biomaterials and anti-inflammatory design—a brief review. Macromol Biosci 2018;18:e1800112. [PubMed: 29920937]
17. Anderson JM. Inflammatory response to implants. ASAIO Trans 1988;34:101–7. [PubMed: 3285869]

18. Morais JM, Papadimitrakopoulos F, Burgess DJ. Biomaterials/tissue interactions: possible solutions to overcome foreign body response. AAPS J 2010;12:188–96. [PubMed: 20143194]
19. Brodbeck WG, Nakayama Y, Matsuda T, et al. Biomaterial surface chemistry dictates adherent monocyte/macrophage cytokine expression in vitro. Cytokine 2002;18:311–9. [PubMed: 12160519]
20. Chen S, Jones JA, Xu Y, et al. Characterization of topographical effects on macrophage behavior in a foreign body response model. Biomaterials 2010;31:3479–91. [PubMed: 20138663]
21. Marques AP, Reis RL, Hunt JA. An in vivo study of the host response to starch-based polymers and composites subcutaneously implanted in rats. Macromol Biosci 2005;5:775–85. [PubMed: 16080170]
22. Baker DW, Liu X, Weng H, et al. Fibroblast/fibrocyte: surface interaction dictates tissue reactions to micropillar implants. Bio-macromolecules 2011;12:997–1005.
23. Zhou G, Loppnow H, Groth T. A macrophage/fibroblast co-culture system using a cell migration chamber to study inflammatory effects of biomaterials. Acta Biomater 2015;26:54–63. [PubMed: 26292266]
24. Ratner BD, Bryant SJ. Biomaterials: where we have been and where we are going. Annu Rev Biomed Eng 2004;6:41–75. [PubMed: 15255762]
25. Hsu WK, Polavarapu M, Riaz R, et al. Characterizing the host response to rhBMP-2 in a rat spinal arthrodesis model. Spine (Phila Pa 1976) 2013;38:E691–8. [PubMed: 23429681]
26. Hsu WK, Wang JC, Liu NQ, et al. Stem cells from human fat as cellular delivery vehicles in an athymic rat posterolateral spine fusion model. J Bone Joint Surg Am 2008;90:1043–52. [PubMed: 18451397]
27. Wang JC, Kanim LE, Yoo S, et al. Effect of regional gene therapy with bone morphogenetic protein-2-producing bone marrow cells on spinal fusion in rats. J Bone Joint Surg Am 2003;85:905–11. [PubMed: 12728043]
28. Driscoll JA, Lubbe R, Jakus AE, et al. 3D-printed ceramic-demineralized bone matrix hyperelastic bone composite scaffolds for spinal fusion. Tissue Eng Part A 2020;26:157–66. [PubMed: 31469055]
29. Hallman M, Driscoll JA, Lubbe R, et al. Influence of geometry and architecture on the in vivo success of 3D-printed scaffolds for spinal fusion. Tissue Eng Part A 2021;271:26–36.
30. Jakus AE, Rutz AL, Jordan SW, et al. Hyperelastic “bone”: a highly versatile, growth factor-free, osteoregenerative, scalable, and surgically friendly biomaterial. Sci Transl Med 2016;8: 358ra127.
31. Hsu WK, Polavarapu M, Riaz R, et al. Nanocomposite therapy as a more efficacious and less inflammatory alternative to bone morphogenetic protein-2 in a rodent arthrodesis model. J Orthop Res 2011;29:1812–9. [PubMed: 21590717]
32. Fedorov A, Beichel R, Kalpathy-Cramer J, et al. 3D Slicer as an image computing platform for the quantitative imaging network. Magn Reson Imaging 2012;30:1323–41. [PubMed: 22770690]
33. Ge Z, Tian X, Heng BC, et al. Histological evaluation of osteogenesis of 3D-printed poly-lactic-co-glycolic acid (PLGA) scaffolds in a rabbit model. Biomed Mater 2009;4:021001. [PubMed: 19208943]
34. Shim JH, Yoon MC, Jeong CM, et al. Efficacy of rhBMP-2 loaded PCL/PLGA/beta-TCP guided bone regeneration membrane fabricated by 3D printing technology for reconstruction of calvaria defects in rabbit. Biomed Mater 2014;9:065006. [PubMed: 25384105]
35. Bose S, Vahabzadeh S, Bandyopadhyay A. Bone tissue engineering using 3D printing. Materials Today 2013;16:496–504.
36. Houchin ML, Topp EM. Chemical degradation of peptides and proteins in PLGA: a review of reactions and mechanisms. J Pharm Sci 2008;97:2395–404. [PubMed: 17828756]
37. Shive MS, Anderson JM. Biodegradation and biocompatibility of PLA and PLGA microspheres. Adv Drug Deliv Rev 1997;28:5–24. [PubMed: 10837562]
38. Subramanian A, Krishnan UM, Sethuraman S. In vivo biocompatibility of PLGA-polyhexylthiophene nanofiber scaffolds in a rat model. Biomed Res Int 2013;2013:390518. [PubMed: 23971031]

39. Babilotte J, Guduric V, Le Nihouannen D, et al. 3D printed polymer-mineral composite biomaterials for bone tissue engineering: fabrication and characterization. J Biomed Mater Res B Appl Biomater 2019;107:2579–95. [PubMed: 30848068]
40. Turnbull G, Clarke J, Picard F, et al. 3D bioactive composite scaffolds for bone tissue engineering. Bioact Mater 2018;3:278–314. [PubMed: 29744467]
41. Xiong C, Daubs MD, Montgomery SR, et al. BMP-2 adverse reactions treated with human dose equivalent dexamethasone in a rodent model of soft-tissue inflammation. Spine (Phila Pa 1976) 2013;38:1640–7. [PubMed: 23715023]
42. Ye S, Yim JH, Kim JR, et al. Effects of Diclofenac Sodium on BMP-induced inflammation in a rodent model. Spine (Phila Pa 1976) 2015;40:E799–807. [PubMed: 26164161]
43. Lee KB, Murray SS, Taghavi CE, et al. Bone morphogenetic protein-binding peptide reduces the inflammatory response to recombinant human bone morphogenetic protein-2 and recombinant human bone morphogenetic protein-7 in a rodent model of soft-tissue inflammation. Spine J 2011;11:568–76. [PubMed: 21729805]
44. Tan Y, Montgomery SR, Aghdasi BG, et al. The effect of corticosteroid administration on soft-tissue inflammation associated with rhBMP-2 use in a rodent model of inflammation. Spine (Phila Pa 1976) 2013;38:806–13. [PubMed: 23197010]
45. Dinarello CA. A clinical perspective of IL-1β as the gatekeeper of inflammation. Eur J Immunol 2011;41:1203–17. [PubMed: 21523780]
46. Kaneko H, Arakawa T, Mano H, et al. Direct stimulation of osteoclastic bone resorption by bone morphogenetic protein (BMP)-2 and expression of BMP receptors in mature osteoclasts. Bone 2000;27:479–86. [PubMed: 11033442]
47. Miyamoto K, Ninomiya K, Sonoda K-H, et al. MCP-1 expressed by osteoclasts stimulates osteoclastogenesis in an autocrine/paracrine manner. Biochem Biophys Res Commun 2009;383:373–7. [PubMed: 19364494]

Key Points

- The substantial host inflammatory response associated with rhBMP-2 has generated significant interest in the development of novel bone graft substitutes with more favorable safety profiles.
- This study evaluates the host inflammatory response to our previously-described 3D-printed HA and DBM composite scaffold, which has shown promise as a bone graft substitute for spinal fusion.
- The HA-DBM implant produced no hyperinflammatory response upon implantation, with edema and cytokine expression levels comparable to an absorbable collagen sponge control in a preclinical spine fusion model; this was in contrast to rhBMP-2, which produced significantly greater inflammation relative to the HA-DBM.

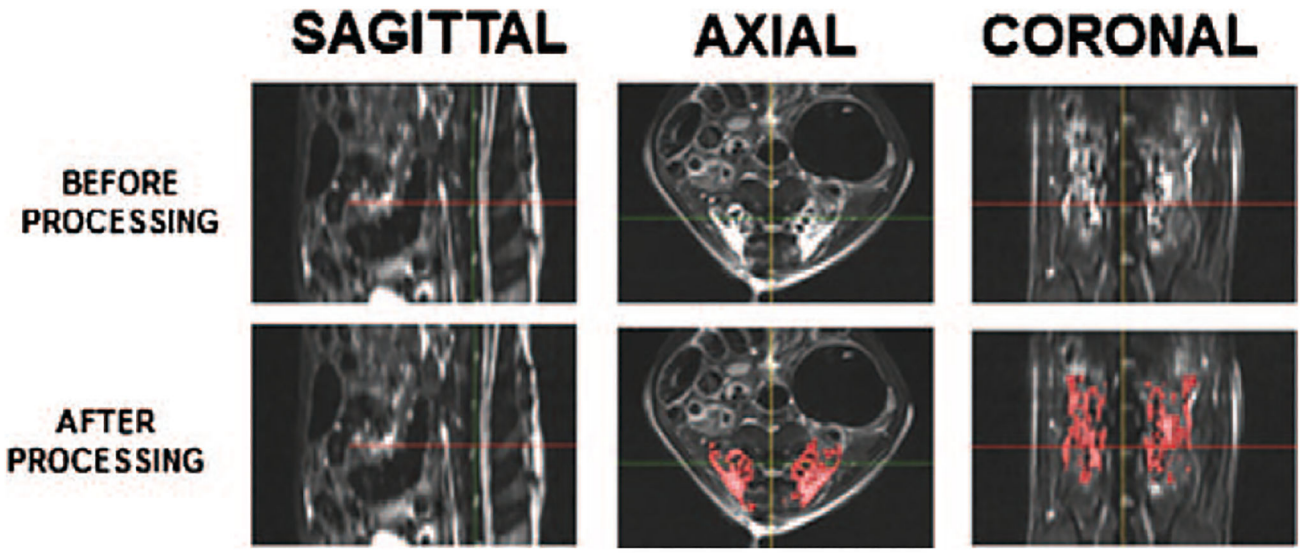

Figure 1.

Depiction of MRI analysis methodology. Sagittal, axial, and coronal views of an HA-DBM implant are provided both before and after processing. Image processing involved isolating the local edema at the surgical site using threshold-based automatic segmentation of standardized MRI images. The local edema was identified (depicted as red overlay) and the total volume of edema was calculated. The crosshair is at the midline, just superior to the L4/L5 disc. HA-DBM indicates hydroxyapatixte-demineralized bone matrix; MRI, magnetic resonance imaging.

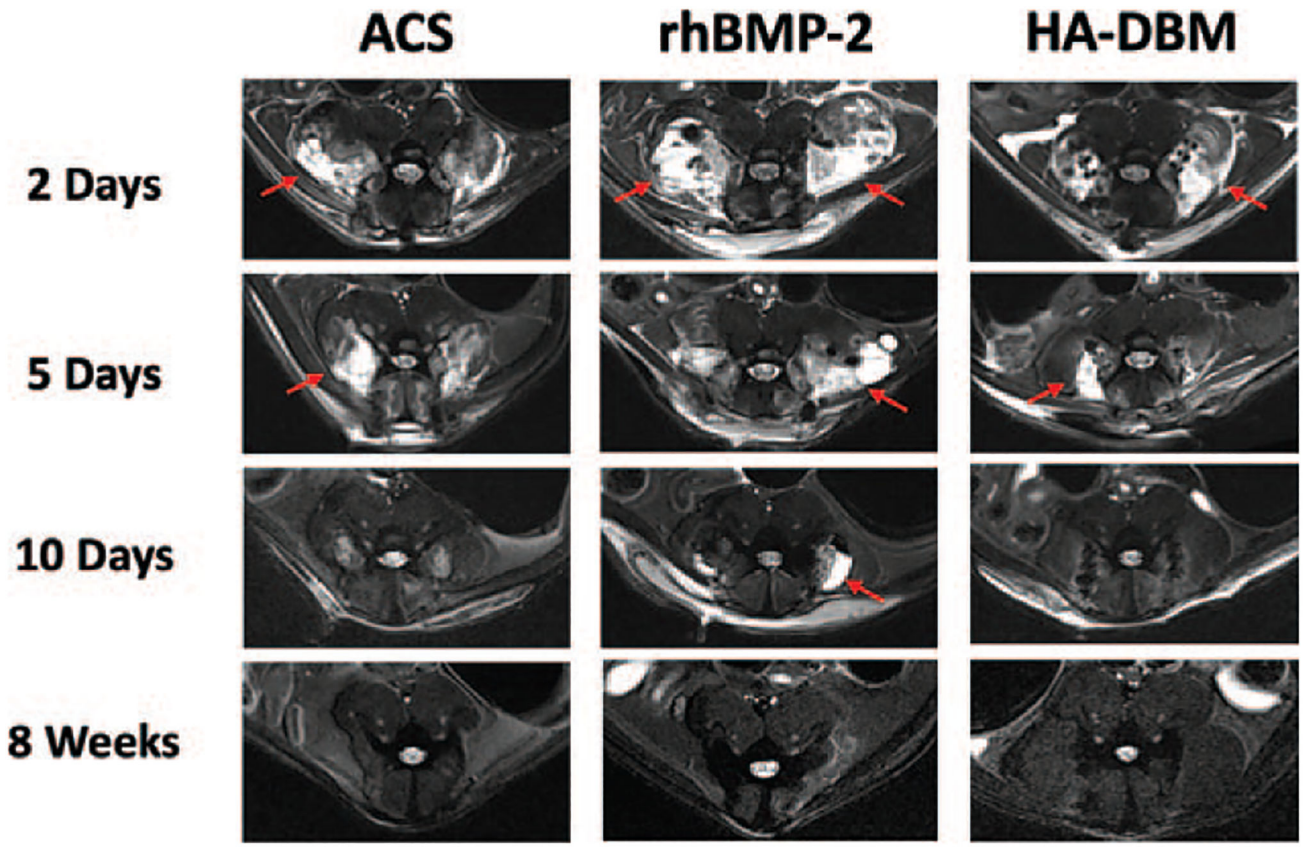

Figure 2.

Representative axial T2-weighted MR images of animal groups at various time points after surgery are shown (N = 5 per treatment group per time point). A large fluid collection (red arrows) was reproducible in those animals receiving rhBMP-2 that was most pronounced at 2 days after surgical implantation and was not typically seen in the ACS and HA-DBM groups. ACS indicates absorbable collagen sponge; DBM, demineralized bone matrix; HA, hydroxyapatite; MR, magnetic resonance; rhBMP-2, recombinant human bone morphogenetic protein-2.

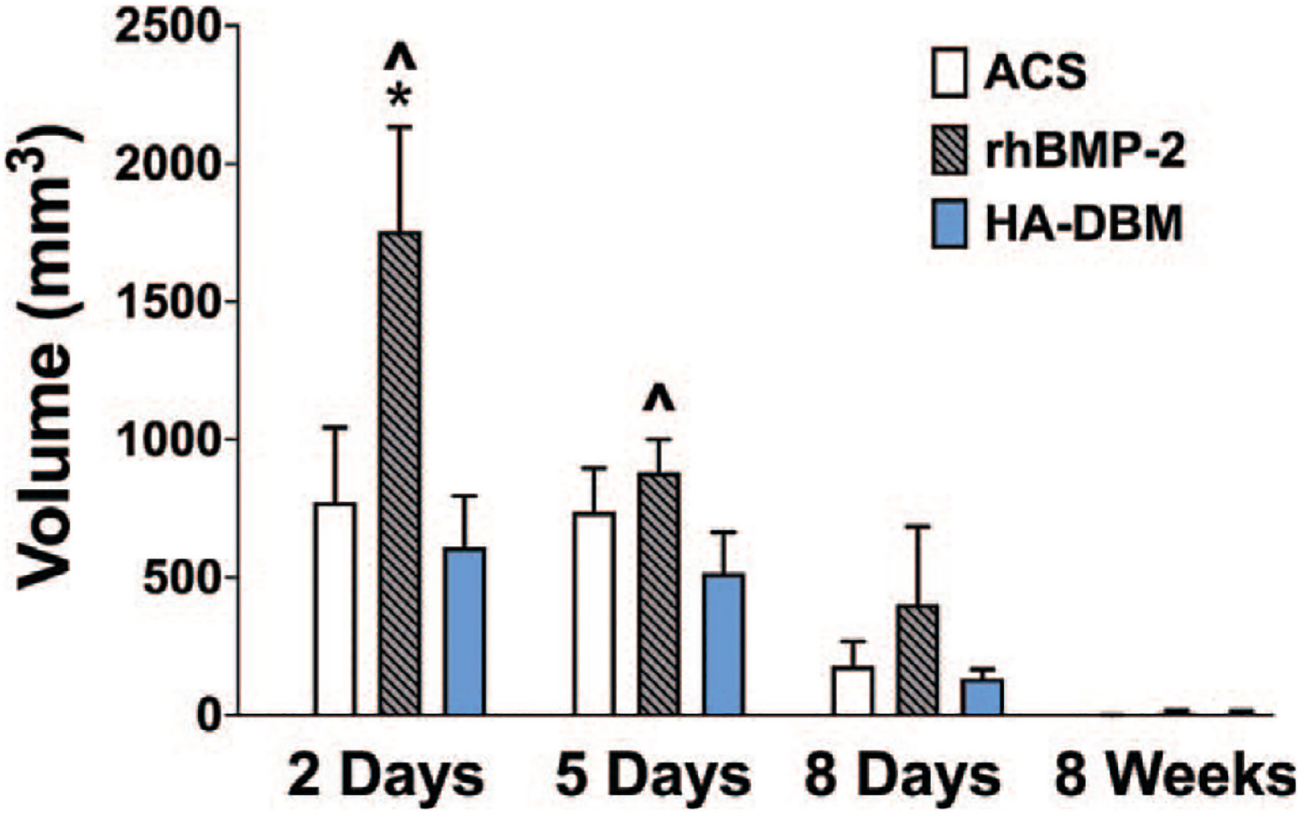

Figure 3.

Quantification of inflammatory edema volume within the fusion bed (intramuscular/subfascial) on axial T2-weighted MR images in all animal groups at 2 days, 5 days, 10days, and 8 weeks postoperatively (N = 5 per treatment group per time point). Significantly greater inflammatory edema volume was measured in the rhBMP-2 group as early as 2 days after surgery when compared with the ACS (*) and HA-DBM (^) groups ($P < 0.05$). ACS indicates absorbable collagen sponge; DBM, demineralized bone matrix; HA, hydroxyapatite; MR, magnetic resonance.

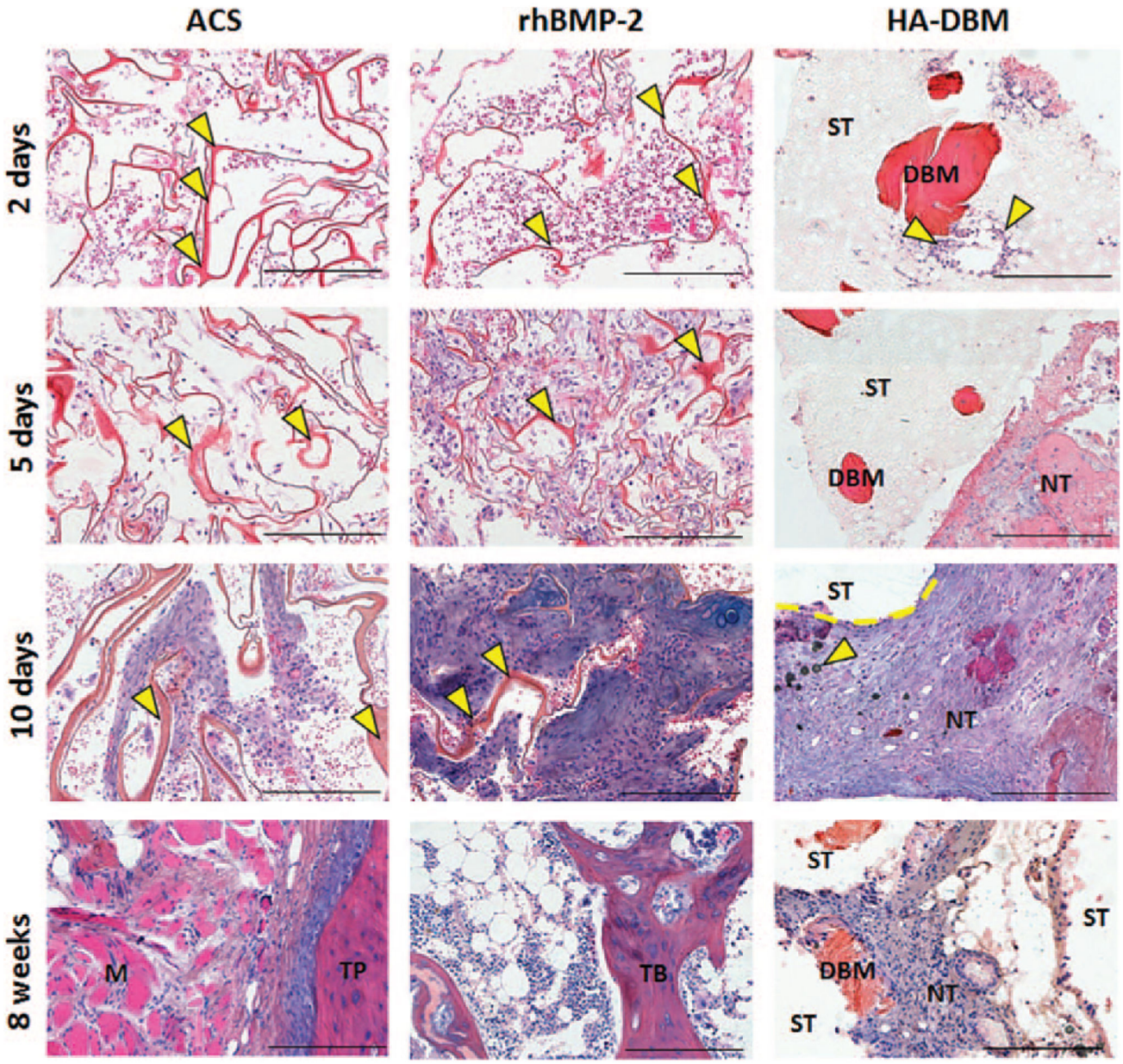

Figure 4.

Histological evaluation of the implants 2, 5, 10 days and 8 weeks postoperatively, stained with Gill's hematoxylin, eosin and alcian blue. Yellow arrows in the ACS and rhBMP-2 samples indicate collagen bundles (red, ribbon-like). Yellow arrows in the 2 days HA-DBM sample indicate cells (purple nuclei) in proximity of a DBM particle. Yellow arrows in the 10 days HA-DBM sample indicate residual HA particles. Legend: Scaffold struts = ST; demineralized bone matrix = DBM; new tissue = NT; muscle M; transverse process = TP; trabecular bone = TB. Scale bars: 400 μm. ACS indicates absorbable collagen sponge; DBM, demineralized bone matrix; HA, hydroxyapatite.

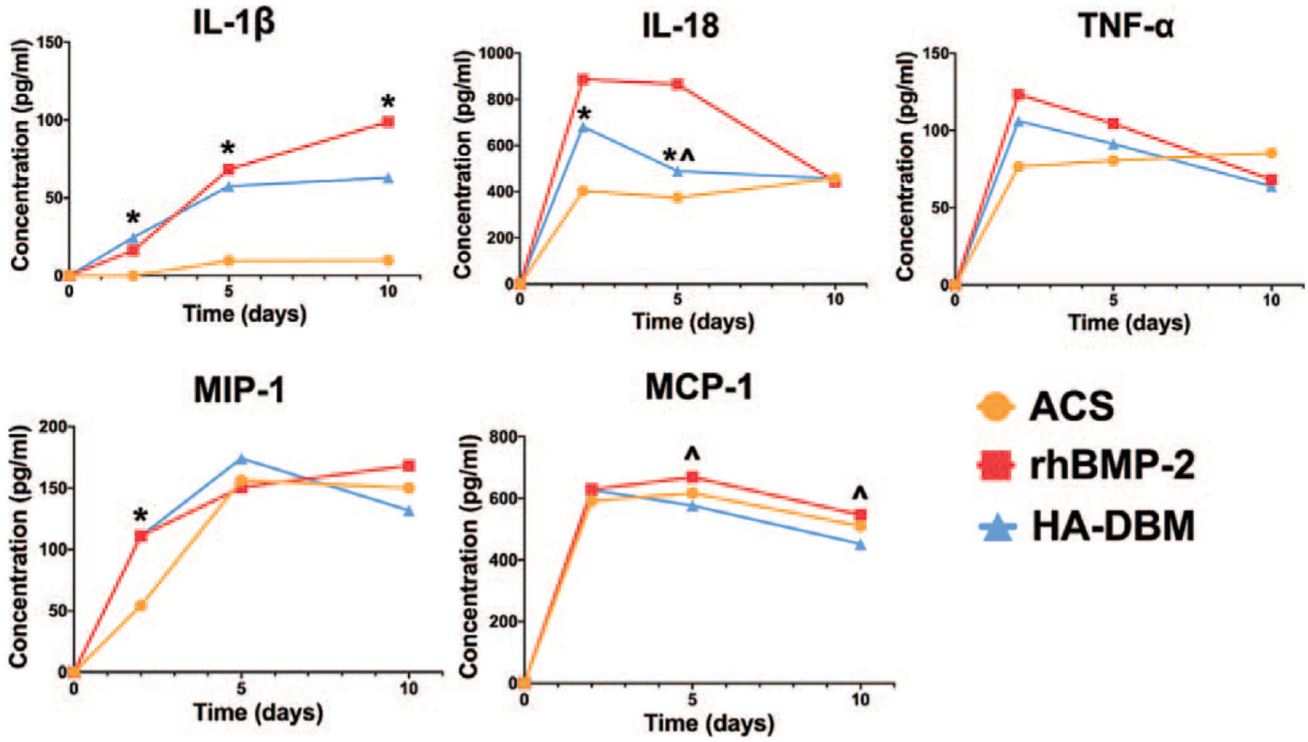

Figure 5.

Serum levels of the following cytokines of interest were quantified longitudinally *via* ELISA (N = 5 per treatment group per time point): IL-1β, IL-18, TNFα, MIP-1, and MCP-1. Levels were compared among animals treated with ACS alone, rhBMP-2/ACS, and HA-DBM scaffolds. Statistical significance for the HA-DBM group relative to ACS alone (*) and rhBMP-2/ACS (^) groups is indicated ($P < 0.05$). ACS indicates absorbable collagen sponge; DBM, demineralized bone matrix; ELISA, enzyme-linked immunosorbent assays; HA, hydroxyapatite.

TABLE 1.

Comparison of the Relative Cytokine Expression Between ACS, rhBMP-2, and HA-DBM Treatment Groups As Determined by ELISA at Days 2, 5, and 10 Postoperatively (N = 5 per Treatment Group per Time Point)

		ACS	rhBMP-2	HA-DBM	*P* (ACS *Versus* rhBMP-2)	*P* (ACS *Versus* HA-DBM)	*P* (rhBMP-2 *Versus* HA-DBM)
IL-1β	Day 2	0.0 ± 0.0	16.2 ± 5.2	24.6 ± 14.5	**0.0343**	**0.0024**	0.3282
	Day 5	9.6 ± 7.2	68.3 ± 41.7	57.4 ± 20.8	**0.0133**	**0.0413**	0.8051
	Day 10	9.9 ± 11.4	98.8 ± 42.8	62.9 ± 14.9		**0.0229**	0.1307
					0.0006		
IL-18	Day 2	402.6 ± 44.6	483.9 ± 133.5	677.2 ± 65.8	0.6907	**0.0226**	0.1369
	Day 5	374.0 ± 57.9	507.1 ± 188.9	865.8 ± 366.3	0.3778	**<0.0001**	**0.0024**
	Day 10	421.2 ± 53.7	456.2 ± 130.0	442.8 ± 41.4	0.9331	0.9738	0.9899
TNF-α	Day 2	82.8 ± 11.6	136.1 ± 39.2	92.9 ± 35.7	**0.0175**	0.8476	0.0631
	Day 5	88.0 ± 29.3	107.1 ± 30.2	91.6 ± 21.5	0.5603	0.9794	0.6807
	Day 10	89.9 ± 13.7	54.3 ± 33.3	61.9 ± 34.7	0.1456	0.2966	0.9102
MIP-1	Day 2	54.3 ± 41.5	111.0 ± 20.5	110.9 ± 27.4	**0.0339**	**0.0342**	>0.999
	Day 5	156.5 ± 24.0	150.7 ± 38.3	174.4 ± 17.8	0.9430	0.5852	0.4032
	Day 10	150.1 ± 29.7	168.5 ± 18.7	131.9 ± 33.5	0.5679	0.5746	0.1390
MCP-1	Day 2	734.2 ± 29.6	847.7 ± 73.9	790.0 ± 75.9	**0.0235**	0.3718	0.3477
	Day 5	763.1 ± 91.3	913.5 ± 77.4	737.7 ± 36.2	**0.0022**	0.8105	**0.0004**
	Day 10	660.0 ± 87.7	711.9 ± 42.5	562.3 ± 23.9	0.4227	0.0572	**0.0023**

Statistical significance is indicated with bolded P values (P<0.05) for all comparisons.